

Direct observation of resonance tryptophan-to-chromophore energy transfer in visible fluorescent proteins

Nina V. Visser^{a,d}, Jan Willem Borst^{a,b}, Mark A. Hink^{a,b},
Arie van Hoek^{a,c}, Antonie J.W.G. Visser^{a,b,e,*}

^aMicroSpectroscopy Centre, Wageningen University, P.O. Box 8128, 6700 ET Wageningen, The Netherlands

^bLaboratory of Biochemistry, Wageningen University, P.O. Box 8128, 6700 ET Wageningen, The Netherlands

^cLaboratory of Biophysics, Wageningen University, P.O. Box 8128, 6700 ET Wageningen, The Netherlands

^dEukaryotic Microbiology, University of Groningen, P.O. Box 14, 9750 AA Haren, The Netherlands

^eDepartment of Structural Biology, Faculty of Earth and Life Sciences, Vrije Universiteit, De Boelelaan 1085, 1081 HV Amsterdam, The Netherlands

Received 8 March 2005; accepted 7 April 2005

Available online 11 May 2005

Abstract

Visible fluorescent proteins from *Aequorea victoria* contain next to the fluorophoric group a single tryptophan residue. Both molecules form a single donor–acceptor pair for resonance energy transfer (RET) within the protein. Time-resolved fluorescence experiments using tryptophan excitation have shown that RET is manifested by a distinct growing in of acceptor fluorescence at a rate characteristic for this process. In addition, time-resolved fluorescence anisotropy measurements under the same excitation–emission conditions showed a correlation time that is similar to the time constant of the same RET process with the additional benefit of gaining information on the relative orientation of the corresponding transition dipoles.

© 2005 Elsevier B.V. All rights reserved.

Keywords: Resonance energy transfer; Green fluorescent protein; Cyan fluorescent protein; Yellow fluorescent protein; Tryptophan; Time-resolved fluorescence; Fluorescence anisotropy

1. Introduction

The green fluorescent protein (GFP) together with its differently coloured mutants has found widespread utilization in cell biology as a natural, brightly fluorescent marker for gene expression, localization of gene products and intracellular protein–protein interaction via resonance energy transfer (reviews: [1–3]). The isolated protein itself is a wonderful optical spectroscopic molecular laboratory. To understand the complex photophysics of GFP and its mutants a considerable number of optical spectroscopic studies have been published ranging from picosecond time-resolved fluorescence [4–8], spec-

tral hole-burning at cryogenic temperature [9,10] to circular dichroism [11]. One aspect of GFP that was not yet studied, to the best of our knowledge, is resonance energy transfer (RET) from the single tryptophan residue to the chromophore making tryptophan fluorescence barely visible in the native protein. According to the 3-dimensional structure of EGFP [12], RET must be very efficient, since the distance between both molecules is only 17 Å (Fig. 1).

In this work we have studied RET using single-photon timing fluorescence spectroscopy selecting both tryptophan and chromophore emissions upon excitation of tryptophan. We could observe a very rapid fluorescence decay of the donor (tryptophan) and a concomitant rise of acceptor (chromophore) fluorescence. In addition, this resonant energy transfer process is examined, for the first time, via monitoring of acceptor fluorescence anisotropy decay upon donor excitation. Both types of experiments require specific

* Corresponding author. MicroSpectroscopy Centre, Laboratory of Biochemistry, Wageningen University, P.O. Box 8128, 6700 ET Wageningen. Tel.: +31 317 482862; fax: +31 317 484801.

E-mail address: ton.visser@wur.nl (A.J.W.G. Visser).

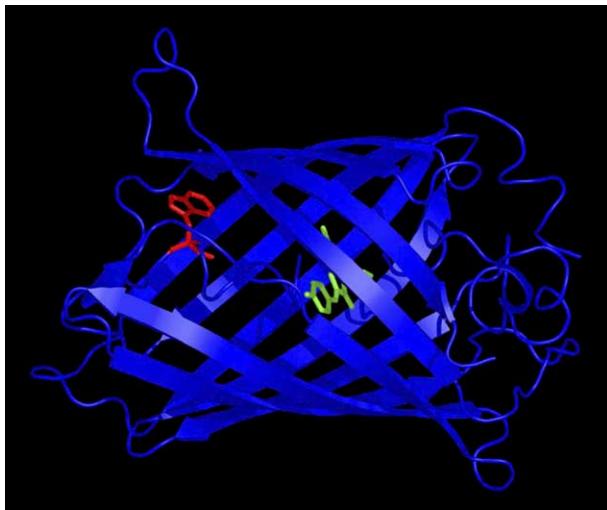


Fig. 1. 3D structure of GFP (blue) with the tryptophan in red and the fluorophore in green. (For interpretation of the references to colour in this figure legend, the reader is referred to the web version of this article.)

global analytical approaches to recover the appropriate decay parameters.

2. Materials and methods

2.1. Protein material, sample preparation and steady-state fluorescence spectroscopy

The enhanced forms of CFP, GFP and YFP were isolated and purified as described in [11]. The visible fluorescent proteins (VFPs) were dissolved in PBS buffer at pH 7.4. The VFPs were diluted to a final concentration of 200 nM. The steady-state fluorescence spectra were obtained with a Spex-Fluorolog 3.2.2 spectrophotometer at 295 K as described in [13]. A quartz cuvette of 1.0×0.4 cm contained the protein solutions. The slits in the double-grating excitation and emission monochromators were 1 nm. Both excitation and emission spectra were corrected by a procedure supplied by the manufacturer and normalized to unity using the maximum values. The spectra were acquired at wavelength steps of 1 nm.

2.2. Time-resolved fluorescence and fluorescence anisotropy measurements

Time-resolved polarized fluorescence experiments were carried out using the time-correlated single-photon counting technique (TCSPC) [14]. The TCSPC setup and the measurement procedures used were described in detail elsewhere [8,15], and will only briefly be outlined below. A mode-locked CW Nd:YLF laser was used for the synchronous pumping of a cavity-dumped, dye laser (Rhodamine 6G) providing after frequency-doubling excitation at 300 nm. The samples were excited with vertically polarized light pulses (4 ps FWHM) at an excitation

frequency of 591 kHz and both parallel and perpendicularly polarized fluorescence were detected. At 300-nm excitation tryptophan fluorescence was detected with a 348.8-nm interference filter (Schott, Mainz, Germany, half-bandwidth of 5.4 nm). At 300-nm excitation, visible fluorescence was detected with a KV470-nm cut-off filter (Schott). The data were collected in a multichannel analyzer with a maximum time window of 4096 channels typically at 5 ps/channel. The dynamic instrumental response function of the setup was approximately 40–50 ps FWHM, and was obtained at the tryptophan emission wavelength using a solution of *p*-terphenyl in cyclohexane, which fluorescence was quenched by CCl₄ (50/50, v/v; $\tau_{\text{ref}}=20$ ps) [16] and at visible emission wavelengths using erythrosine B in water ($\tau_{\text{ref}}=80$ ps) [17] as reference compounds. One complete experiment for a fluorescence decay measurement consisted of the recording of data sets of the reference compound, the VFP sample, the background (buffer) and again the reference compound.

2.3. Data analysis

Data analysis was performed using a model of discrete exponential terms. Global analysis of the experimental data was performed using the ‘TRFA Data Processing Package’ of the Scientific Software Technologies Center (Belarusian State University, Minsk, Belarus) [18,19]. The total fluorescence intensity decay $I(t)$ was obtained from the measured parallel $I_{\parallel}(t)$ and perpendicular $I_{\perp}(t)$ fluorescence intensity components through the relation:

$$I(t) = I_{\parallel}(t) + 2I_{\perp}(t) \quad (1)$$

The fluorescence lifetime profile consisting of a sum of discrete exponentials with lifetime τ_i and amplitude α_i can be retrieved from the total fluorescence $I(t)$ through the convolution product:

$$I(t) = E(t) \otimes \sum_{i=1}^N \alpha_i e^{-t/\tau_i} \quad (2)$$

where $E(t)$ is the instrumental response function.

The anisotropy decay $r(t)$ is given by the following relation:

$$r(t) = \frac{I_{\parallel}(t) - I_{\perp}(t)}{I_{\parallel}(t) + 2I_{\perp}(t)} \quad (3)$$

In fluorescence anisotropy analysis, after deconvolution, the time-dependent fluorescence anisotropy $r(t)$ is calculated from the parallel $I_{\parallel}(t)$ and perpendicular $I_{\perp}(t)$ components through the relations [20]:

$$I_{\parallel}(t) = \frac{1}{3} \sum_{i=1}^N \alpha_i e^{-t/\tau_i} \left\{ 1 + 2 \sum_{j=1}^M r_{0j} e^{-t/\phi_j} \right\} \quad (4)$$

$$I_{\perp}(t) = \frac{1}{3} \sum_{i=1}^N \alpha_i e^{-t/\tau_i} \left\{ 1 - \sum_{j=1}^M r_{0j} e^{-t/\phi_j} \right\} \quad (5)$$

in which $i=j$ for correlated systems in which particular lifetime components τ_i are associated with particular correlation times ϕ_i (correlated or associative model), and $i \neq j$ for systems in which all lifetimes equally contribute to the anisotropy (uncorrelated or nonassociative model); r_0 is the fundamental anisotropy at time $t=0$. In addition, a rigorous error analysis at the 67% confidence level was applied to the optimized fluorescence lifetimes and rotational correlation times [21].

3. Results and discussion

3.1. Steady-state excitation and emission spectra of VFPs

In Fig. 2 the steady-state fluorescence emission and excitation spectra of all three VFPs have been collected. These spectra serve to illustrate that the spectra are dominated by the spectral properties of the fluorophores in the visible spectrum. When the fluorescence emission spectra obtained at 300-nm excitation are compared (Fig. 2A), the quenched fluorescence emission of the tryptophan residue around 340 nm can be barely distinguished. The corrected excitation spectra are displayed in Fig. 2B. The large contribution of the chromophore of ECFP in the region 250–310 nm is very apparent. The reason for this is that indole is also a constituent of the chromophoric group in

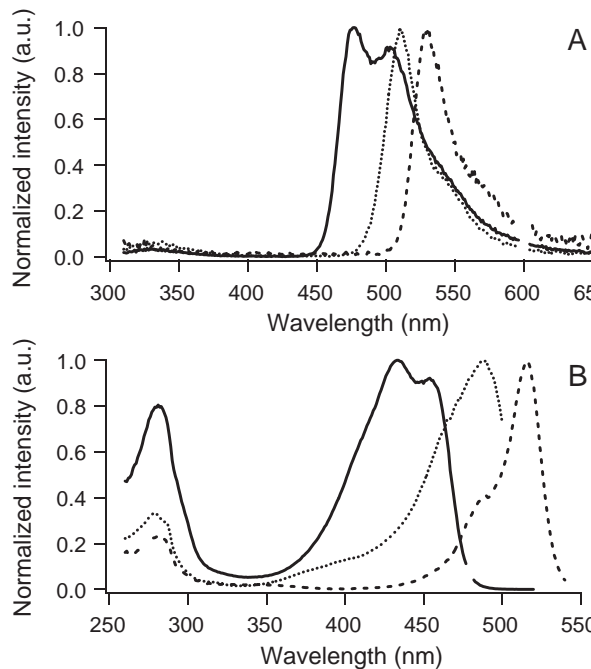


Fig. 2. Corrected fluorescence emission and excitation spectra of ECFP, EGFP and EYFP. A. Fluorescence emission spectra obtained upon excitation at 300 nm in the range 310–650 nm of ECFP (solid line), EGFP (dotted line) and EYFP (dashed line). The second order scattering at 600 nm has been removed in all spectra. B. Fluorescence excitation spectra of ECFP (solid line, $\lambda_{\text{em}}=480$ nm), EGFP (dotted line, $\lambda_{\text{em}}=510$ nm) and EYFP (dashed line, $\lambda_{\text{em}}=550$ nm).

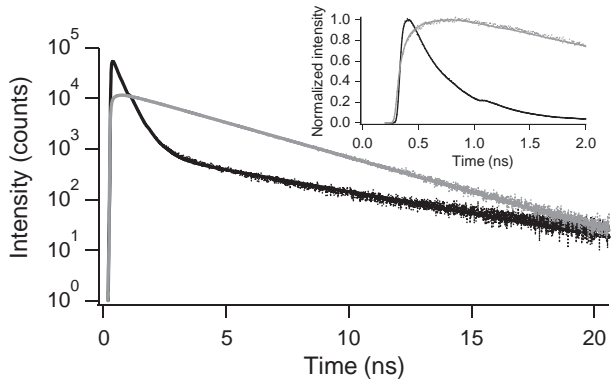


Fig. 3. Experimental (dotted line) and fitted (solid line) fluorescence decay curves of the tryptophan residue (black) and the fluorophore (gray) in green fluorescent protein. The excitation wavelength for both fluorophores was 300 nm. The detection wavelength for Trp fluorescence was 348.8 nm and for the fluorophore at wavelengths longer than 470 nm. The recovered parameters (α_i, τ_i) are collected in Table 1. The inset shows an enlarged view of the traces between 0 and 2 ns.

ECFP and therefore the chromophoric group absorbs a large part of the 300-nm excitation light.

3.2. Decay of donor fluorescence and increase of acceptor fluorescence: RET verification

In Fig. 3 experimental and fitted fluorescence decay curves of the single tryptophan residue in EGFP are shown. A two-component fit with lifetimes of 0.30 ns and 4.4 ns gave a satisfactory fit. The longest lifetime of 4.4 ns has the smallest amplitude: ~1%. We assign this long lifetime to a protein population in which the chromophoric group was not successfully developed. In other words, there will be no energy transfer from tryptophan to the acceptor. Owing to the large dynamic range of intensities available with the single-photon timing technique, this small population of protein molecules without chromophore, co-purified with normal GFP molecules, can be accurately determined. This relatively simple decay analysis of the donor (Trp) fluorescence allows determining the transfer efficiency E from:

$$E = 1 - \tau_D/\tau_D^0 \quad (6)$$

where the τ_D is the fluorescence lifetime of the donor in the presence of acceptor and the superscript 0 indicates the absence of the acceptor. Substitution of the values of 0.30 ns and 4.4 ns into Eq. (6) yields an efficiency $E=0.94$. Since the distance R between donor and acceptor is known (17 Å), we can obtain the critical transfer distance R_0 from the following relation:

$$R_0 = R \times \{E/(1-E)\}^{1/6} \quad (7)$$

leading to $R_0=27$ Å.

In Fig. 3 also the time-dependence of the acceptor fluorescence upon donor excitation has been presented. By expanding the time scale (inset Fig. 3) it can be clearly

observed that the acceptor fluorescence shows first a rise followed by decay. Actually, the transfer rate constant can also be determined from the rise of the acceptor fluorescence following pulse excitation of the donor [22]. Assuming that there is no direct excitation of the acceptor and both acceptor and donor decays are single exponential with lifetimes τ_A and τ_D (note that τ_D is the fluorescence lifetime of the donor in the presence of acceptor), respectively, the time dependence of the fluorescence intensity of the acceptor takes the following form:

$$I_A(t) = A \left[e^{-t/\tau_A} - e^{-t/\tau_D} \right]$$

$$A = \frac{[D^*]_0 k_T}{1/\tau_D - 1/\tau_A} \quad (8)$$

where $[D^*]_0$ is the excited donor concentration at time $t=0$ and k_T is the transfer rate constant. The negative term corresponds to the rise of acceptor fluorescence with a time constant that is equal to the fluorescence lifetime of the donor. In most cases there is also direct excitation of the acceptor at the excitation wavelength of the donor affecting only the pre-exponential factors, but not the lifetimes:

$$I_A(t) = Be^{-t/\tau_A} - Ae^{-t/\tau_D}$$

$$B = A + [A^*]_0 \quad (9)$$

where $[A^*]_0$ is the concentration of directly excited acceptors at time $t=0$.

We have globally analysed decay curves of two different sets of experiments, in which the short lifetimes of the tryptophan fluorescence (τ_D) and the rise of the acceptor fluorescence as well as the long lifetime of EGFP (τ_A) were linked. The fitted curves are also shown in Fig. 3. All parameter values and the confidence limits of the lifetimes are collected in Table 1.

In case of EYFP and ECFP the relative contribution of the long Trp lifetime component is much smaller than for EGFP (see Table 1). The confidence limits are therefore larger. The short lifetime components are slightly shorter than found for EGFP. The relative amplitudes of the acceptor decay fulfil the relationship of Eq. (9) indicating that the chromophore is also directly excited at 300 nm. The degree of direct excitation is largest in case of ECFP, which

can be explained by the nature of the chromophoric group containing an indole moiety similar as in tryptophan. The fluorescence decay of ECFP is clearly biexponential with two lifetime components that are identical to the ones found on direct excitation [23]. This biexponential decay is explained by structural heterogeneity of the chromophoric group within the protein [24].

3.3. Quantitative description of fluorescence emission spectra using information from time-resolved fluorescence

From the amplitudes recovered by analysis of the time-resolved fluorescence of the acceptor upon donor excitation, one can immediately obtain the fraction of directly excited acceptor and the complementary fraction of acceptor that is excited via RET from tryptophan (see Eq. (9) and amplitudes collected in Table 1). These indirect fractions are 0.163 for ECFP, 0.277 for EGFP and 0.243 for EYFP. The contribution of indirectly excited acceptor in the emission spectrum can then be obtained by multiplying the respective fluorescence spectrum with the particular fraction of RET-excited acceptor (range 450–650 nm in Fig. 2A). By comparing integrated intensities of both emission bands a rough indication of the relative quantum yields can be obtained. The integrated intensity of the fluorophore emission spectrum is multiplied by this particular fraction and divided by the integrated intensity of the tryptophan emission spectrum (range 310–400 nm) in the visible fluorescent protein. The relative quantum yield ratio of the fluorophore and tryptophan in ECFP is 7.7, in EGFP 4.7 and in EYFP 5.7.

3.4. Analysis of time-dependent fluorescence anisotropy of acceptor in case of RET

When the time-dependence of the fluorescence anisotropy of EGFP ($\lambda_{\text{exc}}=300$ nm, $\lambda_{\text{em}}>470$ nm) is observed, a characteristic fast decay superimposed on a slow decay is observed (Fig. 4). To obtain a good fit associated decay analysis was necessary, in which the short fluorescence lifetime is associated with a short correlation time and the long fluorescence lifetime with a long correlation time (see fitted curve in Fig. 4). The short fluorescence lifetime originates from energy transfer and therefore the short

Table 1

Fluorescence decay parameters of tryptophan and fluorophore in visible fluorescent proteins upon excitation at 300 nm

Monitoring	α_1 (-)	τ_1 (ns)	α_2 (-)	τ_2 (ns)	α_3 (-)	τ_3 (ns)
Trp in EGFP	0.986	0.307 (0.295–0.308)	0.014	4.5 (4.3–4.6)	n.a.	n.a.
EGFP	-0.277	0.307 (0.295–0.308)	1.0	3.09 (3.09–3.10)	n.a.	n.a.
Trp in EYFP	0.999	0.240 (0.239–0.241)	0.001	5.3 (4.4–6.6)	n.a.	n.a.
EYFP	-0.243	0.240 (0.239–0.241)	1.0	3.81 (3.80–3.84)	n.a.	n.a.
Trp in ECFP	0.999	0.206 (0.206–0.209)	0.001	6.3 (5.4–7.9)	n.a.	n.a.
ECFP	-0.163	0.206 (0.206–0.209)	0.368	1.20 (0.93–1.48)	0.632	3.81 (3.72–3.93)

Values in parentheses are the confidence limits obtained after a rigorous error analysis at the 67% confidence level.

n.a. not applicable.

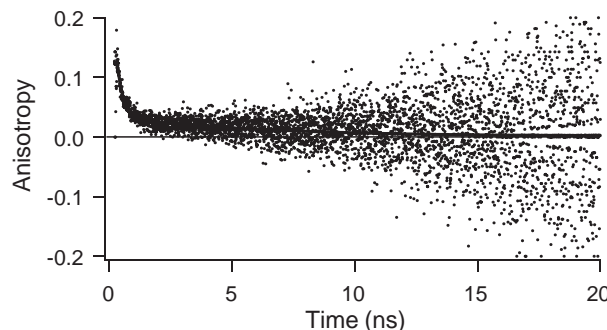


Fig. 4. Experimental (dots) and fitted (solid line) fluorescence anisotropy decay of green fluorescent protein upon excitation at 300 nm and monitoring the fluorophore at wavelengths >470 nm. The associative analysis yielded correlation times (ϕ_i) and amplitudes (β_i) that are collected in Table 2.

correlation time must also arise from energy transfer. The short correlation time can be considered as a time constant of reorientation of the donor dipole to acceptor dipole during the energy transfer process. All parameters recovered from global analysis are collected in Table 2. Since the chromophore is rigidly attached within the protein matrix the long correlation time must be due to the rotational correlation time of the whole protein. For EGFP and EYFP the correlation times seem to be somewhat smaller than when the fluorophore is directly excited [8,23]. It should be realized, however, that the corresponding amplitudes are almost a factor of 10 smaller than when directly excited (see Table 2). Therefore the long correlation times are less accurate. According to time-resolved fluorescence anisotropy monitoring the emission at 349 nm the tryptophan residue is also rigidly attached in the protein structure (results not shown).

The difference between the pre-exponential amplitudes β_i of the fast anisotropy decay can be related to geometrical parameters describing the relative orientation of indole and chromophoric group [17]:

$$\beta_1 - \beta_2 = \frac{3}{5} \cos^2 \theta - \frac{1}{5} \quad (10)$$

θ is now the intermolecular angle between the emission transition moment of the tryptophan residue and the absorption transition moment of the chromophore. Assum-

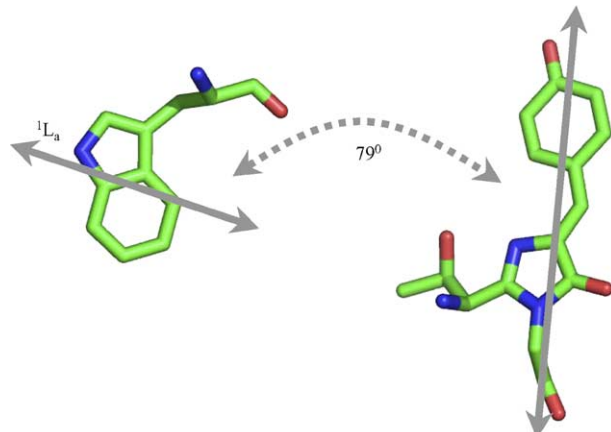


Fig. 5. Relative direction of the transition moments in tryptophan and fluorophore obtained from the amplitudes (β_1 and β_2 , see Table 2) and Eq. (10). The geometry of both molecular structures is obtained from the 3D structure.

ing that the emission transition moment of Trp coincides with the ${}^1\text{L}_\alpha$ transition we can then determine the absorption transition moment in the ring of the chromophore from the obtained value of θ . For EGFP $\theta=79^\circ$, for EYFP $\theta=81^\circ$ and for ECFP $\theta=81^\circ$. The meaning of θ is graphically depicted for EGFP in Fig. 5. It should be noted that the recovered angle is in very good agreement with the relative orientations of the molecular structures within the protein.

4. Conclusions

We have provided evidence from time-resolved fluorescence spectroscopy for resonance energy transfer from the single tryptophan residue to the fluorophoric group in visible fluorescent proteins. A novel element in this study is that we did not make use of measuring tryptophan fluorescence in the absence of the acceptor, which is always necessary for experimental determination of the transfer efficiency. We employed the large dynamical range of the single-photon timing method to detect a protein population in which the fluorophore was not developed. In addition, the use of time-resolved fluorescence anisotropy upon donor

Table 2

Fluorescence (α_i , τ_i) and anisotropy (β_i , ϕ_i) decay parameters of the fluorophore in visible fluorescent proteins (VFP) upon excitation at 300 nm recovered after associated analysis

VFP	α_1 (-)	τ_1 (ns)	β_1 (-)	ϕ_1 (ns)	α_2 (-)	τ_2 (ns)	β_2 (-)	ϕ_2 (ns)	α_3 (-)	τ_3 (ns)
EGFP	-0.26	0.23 (0.19–0.25)	0.095 (0.092–0.097)	0.23 (0.22–0.24)	1.0	3.13 (3.11–3.15)	0.031 (0.030–0.032)	6.5 (6.0–7.0)	n.a.	n.a.
EYFP	-0.25	0.22 (0.19–0.26)	0.082 (0.079–0.085)	0.21 (0.20–0.23)	1.0	3.81 (3.77–3.82)	0.047 (0.046–0.048)	9.2 (8.8–9.7)	n.a.	n.a.
ECFP	-0.19	0.14 (0.09–0.19)	0.054 (n.f.–0.076)	0.22 (0.05–0.33)	0.36	1.26 (1.12–1.38)	0.028 (0.022–0.031)	13.9 (8.2–n.f.)	0.64	3.81 (3.74–3.84)

Values in parentheses are the confidence limits obtained after a rigorous error analysis at the 67% confidence level.
n.a. not applicable; n.f. not found.

In case of ECFP the contribution of ϕ_3 associated with τ_3 was very small.

excitation and detection of acceptor emission and concomitant associative analysis resulted in a correlation time that reflects the rate of energy transfer and in a relative amplitude that provides orientation information on both donor and acceptor molecules. In this way the orientation factor in resonance energy transfer that is unknown in most cases, can be determined [25]. The procedure as outlined in this paper for intra-protein RET measurements can be easily expanded to inter-protein RET, for instance in the genetically encoded fluorescent indicators for measuring intracellular calcium [26–28].

Acknowledgements

We thank Adrie Westphal for providing the 3D graphics of Green Fluorescent Protein.

References

- [1] R.Y. Tsien, The green fluorescent protein, *Ann. Rev. Biochem.* 67 (1998) 509–544.
- [2] J. Lippincott-Schwartz, E. Snapp, A. Kenworthy, Studying protein dynamics in living cells, *Nat. Rev., Mol. Cell Biol.* 2 (2001) 444–456.
- [3] M.A. Hink, T. Bisseling, A.J.W.G. Visser, Imaging protein–protein interactions in living cells, *Plant Mol. Biol.* 50 (2002) 871–882.
- [4] G. Striker, V. Subramanian, C.A.M. Seidel, A. Volkmer, Photochromicity and fluorescence lifetimes of green fluorescent protein, *J. Phys. Chem., B* 103 (1999) 8612–8617.
- [5] A. Volkmer, V. Subramanian, D.J.S. Birch, T.M. Jovin, One- and two-photon excited fluorescence lifetimes and anisotropy decays of green fluorescent proteins, *Biophys. J.* 78 (2000) 1589–1598.
- [6] M. Cotlet, J. Hofkens, M. Maus, T. Gensch, M. Van der Auweraer, J. Michiels, G. Dirix, M. Van Guyse, J. Vanderleyden, A.J.W.G. Visser, F.C. De Schryver, Excited-state dynamics in the enhanced green fluorescent protein mutant probed by picosecond time-resolved single photon counting spectroscopy, *J. Phys. Chem., B* 105 (2001) 4999–5006.
- [7] K. Suhling, J. Siegel, D. Phillips, P.M.W. French, S. Lévéque-Fort, S.E.D. Webb, D.M. Davis, Imaging the environment of green fluorescent protein, *Biophys. J.* 83 (2002) 3589–3595.
- [8] M.A. Uskova, J.W. Borst, A. van Hoek, A. Schots, N.L. Klyachko, A.J.W.G. Visser, Fluorescence dynamics of green fluorescent proteins in AOT reversed micelles, *Biophys. Chem.* 87 (2000) 73–84.
- [9] T.M.H. Creemers, A.J. Lock, V. Subramanian, T.M. Jovin, S. Völker, Three photoconvertible forms of green fluorescent protein identified by spectral hole burning, *Nat. Struct. Biol.* 6 (1999) 557–560.
- [10] T.M.H. Creemers, A.J. Lock, V. Subramanian, T.M. Jovin, S. Völker, Photophysics and optical switching in green fluorescent protein mutants, *Proc. Natl. Acad. Sci. U. S. A.* 97 (2000) 2974–2978.
- [11] N.V. Visser, M.A. Hink, J.W. Borst, G.N.M. van der Krogt, A.J.W.G. Visser, Circular dichroism spectroscopy of fluorescent proteins, *FEBS Lett.* 521 (2002) 31–35.
- [12] M. Ormö, A.B. Cubitt, K. Kallio, L.A. Gross, R.Y. Tsien, S.J. Remington, Crystal structure of the *Aequorea victoria* green fluorescent protein, *Science* 273 (1996) 1392–1395.
- [13] M.A. Hink, N.V. Visser, J.W. Borst, A. van Hoek, A.J.W.G. Visser, Practical use of corrected fluorescence excitation and emission spectra of fluorescent proteins in Förster Resonance Energy Transfer (FRET) studies, *J. Fluoresc.* 13 (2003) 185–188.
- [14] D.V. O'Connor, D. Phillips, *Time-correlated Single Photon Counting*, Academic Press, London, 1984.
- [15] A.J. Kungl, N.V. Visser, A. van Hoek, A.J.W.G. Visser, A. Billich, A. Schilk, H. Gstach, M. Auer, Time-resolved fluorescence anisotropy of HIV-1 protease inhibitor complexes correlates with inhibitor activity, *Biochemistry* 37 (1998) 2778–2786.
- [16] N.V. Visser, A.J.W.G. Visser, T. Konc, P. Kroh, A. van Hoek, New reference compound with single, ultrashort lifetime for time-resolved tryptophan experiments, *Proc. SPIE* 2137 (1994) 618–626.
- [17] P.I.H. Bastiaens, A. van Hoek, J.A.E. Benen, J.C. Brochon, A.J.W.G. Visser, Conformational dynamics and intersubunit energy transfer in wild-type and mutant lipoamide dehydrogenase from *Azotobacter vinelandii*. A multidimensional time-resolved polarized fluorescence study, *Biophys. J.* 63 (1992) 839–853.
- [18] A.V. Digris, V.V. Skakun, E.G. Novikov, A. van Hoek, A. Claiborne, A.J.W.G. Visser, Thermal stability of a flavoprotein assessed from associative analysis of polarized time-resolved fluorescence spectroscopy, *Eur. Biophys. J.* 28 (1999) 526–531.
- [19] P.A.W. van den Berg, A. van Hoek, A.J.W.G. Visser, Evidence for a novel mechanism of time-resolved flavin fluorescence depolarization in glutathione reductase, *Biophys. J.* 87 (2004) 2577–2586.
- [20] J.R. Lakowicz, *Principles of Fluorescence Spectroscopy*, 2nd ed., Kluwer Academic/Plenum Publishers, New York, 1999, (Chapter 11).
- [21] J.M. Beechem, E. Gratton, M. Ameloot, J.R. Knutson, L. Brand, The global analysis of fluorescence intensity and anisotropy decay data: second generation theory and programs, in: J.R. Lakowicz (Ed.), *Topics in fluorescence spectroscopy*, Plenum, New York, 1991, pp. 241–305.
- [22] B. Valeur, *Molecular Fluorescence. Principles and Applications*, Wiley-VCH, Weinheim, 2002, (Chapter 9).
- [23] J.W. Borst, M.A. Hink, A. van Hoek, A.J.W.G. Visser, Effects of refractive index and viscosity on fluorescence and anisotropy decays of enhanced cyan and yellow fluorescent proteins, *J. Fluoresc.* 15 (2005) 153–160.
- [24] J. Hyun Bae, M. Rubini, G. Jung, G. Wiegand, M.H.J. Seifert, M.K. Azim, J.-S. Kim, A. Zumbusch, T.A. Holak, L. Moroder, R. Huber, N. Budisa, Expansion of the genetic code enables design of a novel “gold” class of green fluorescent proteins, *J. Mol. Biol.* 328 (2003) 1071–1081.
- [25] R.E. Dale, J. Eisinger, W.E. Blumberg, The orientational freedom of molecular probes. The orientation factor in intramolecular energy transfer, *Biophys. J.* 26 (1979) 161–193.
- [26] A. Miyawaki, J. Llopis, R. Heim, J.M. McCaffery, J.A. Adams, M. Ikura, R.Y. Tsien, Fluorescent indicators for Ca^{2+} based on green fluorescent proteins and calmodulin, *Nature* 388 (1997) 882–887.
- [27] A. Miyawaki, O. Griesbeck, R. Heim, R.Y. Tsien, Dynamic and quantitative Ca^{2+} measurements using improved cameleons, *Proc. Natl. Acad. Sci. U. S. A.* 96 (1999) 2135–2140.
- [28] S. Habuchi, M. Cotlet, J. Hofkens, G. Dirix, J. Michiels, J. Vanderleyden, V. Subramanian, F.C. De Schryver, Resonance energy transfer in a calcium concentration-dependent cameleon protein, *Biophys. J.* 83 (2002) 3499–3506.